

Jason L. Pippitt^{1,3,*}, David B. Wolff², Walter Petersen², and David A. Marks^{2,3}
 1 NASA Goddard Space Flight Center, Greenbelt, Maryland
 2 NASA Wallops Flight Facility, Wallops Island, Virginia
 3 Science Systems & Applications, Inc, Lanham, Maryland

1. INTRODUCTION

The Global Precipitation Measurement (GPM) Mission satellite and international mission led by NASA and JAXA was launched from Tanegashima, Japan on February 27, 2014. For validation support, an extensive network currently consisting of 78 dual-polarimetric weather radars in different meteorological regimes were selected by the GPM GV (ground validation) program to identify biases between ground observations and satellite retrievals, to assess the physical basis for uncertainties, and to improve both ground and space-based retrievals of precipitation. Remote sensing by ground radars is a key element in bridging the space and time gap between satellite observations and in-situ surface

instrumentation such as rain gauges and disdrometers. A majority of the radars (NOAA WSR-88D) were selected from the eastern United States to coincide geographically with products from the NOAA/NSSL ground-based National Mosaic and Multi-Radar Multi-sensor Quantitative Precipitation Estimation (NMQ/MRMS). Additional radars are located on Pacific islands (Kwajalein Atoll - KPOL; Guam - PGUA; Hawaii – PHMO; PHKI), two Alaskan sites (PAIH; PAEC), one Pacific Northwest site (KLGX) and Puerto Rico (TJUA). There are two S-band dual-polarized research radars in the network, the transportable NASA polarimetric (NPOL) radar and the CHILL radar (CSU – Greely, CO). NPOL data are available from its semi-permanent Mid-Atlantic coastal location near Wallops Flight Facility (Wallops Island, VA) and GPM field campaign locations (MC3E - Ponca City, OK; IFloodS - Traer, IA; IPHEX - Rutherfordton, NC and OLYMPEX – Pacific Beach,

* Corresponding author address: Jason L. Pippitt, GPM-GV, NASA Goddard Space Flight Center, Code 612 Greenbelt, MD 20771; e-mail: jason.l.pippitt@nasa.gov

GPM-GV Radar Sites

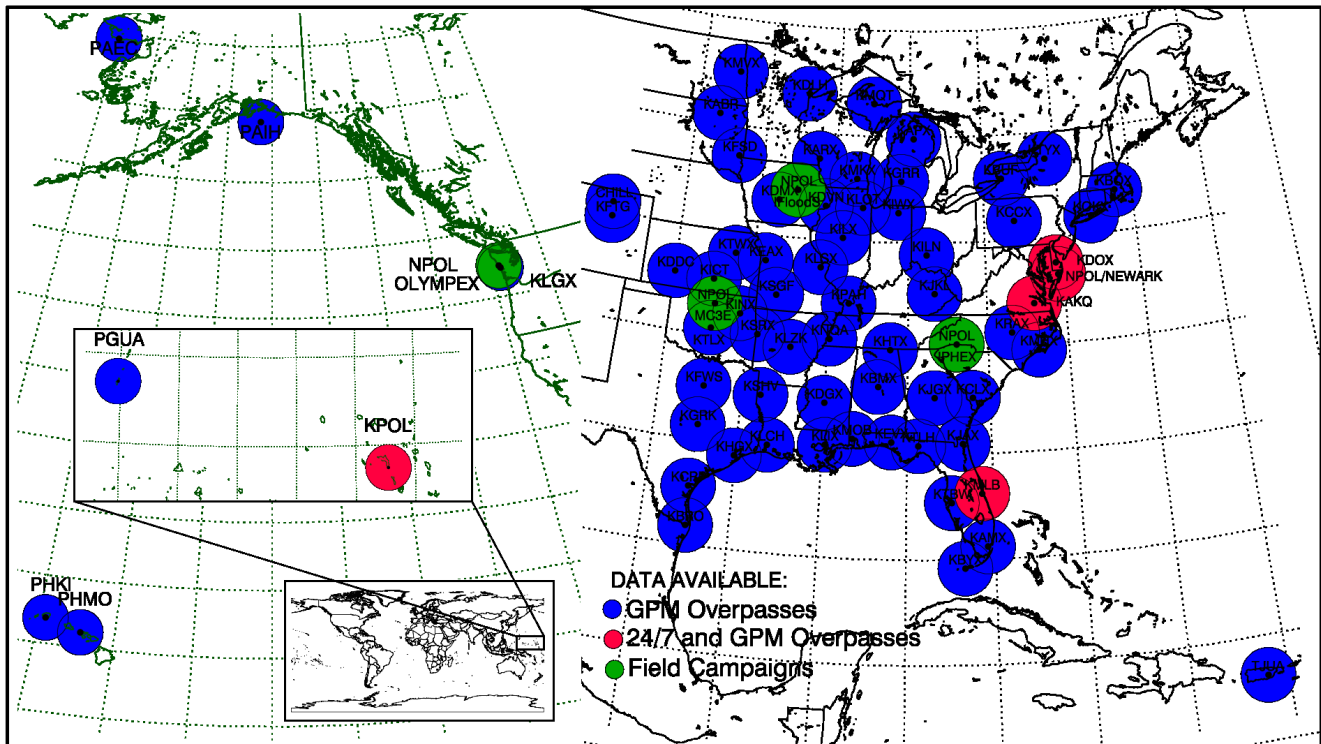


Fig 1. Northern hemisphere GPM-GV radar sites. Blue indicates sites where only GPM overpass data are processed. Red indicates sites where the full daily data sets are processed. Green indicates field campaign sites, which are fully processed.

WA) (Fig. 1). Through an international partnership with Brazil, nine S-band radars from the Center for Monitoring and Alerts of Natural Disasters (CEMADEN) network are included in the GPM GV network (Fig. 2). The Australian Bureau of Meteorology (BOM) CP-2 radar in Brisbane, Australia and several Korean Meteorological Administration (KMA) radars are part of the GPM GV network, the processing of these data sets are conducted in their origin countries.

GPM-GV Brazilian Radar Sites

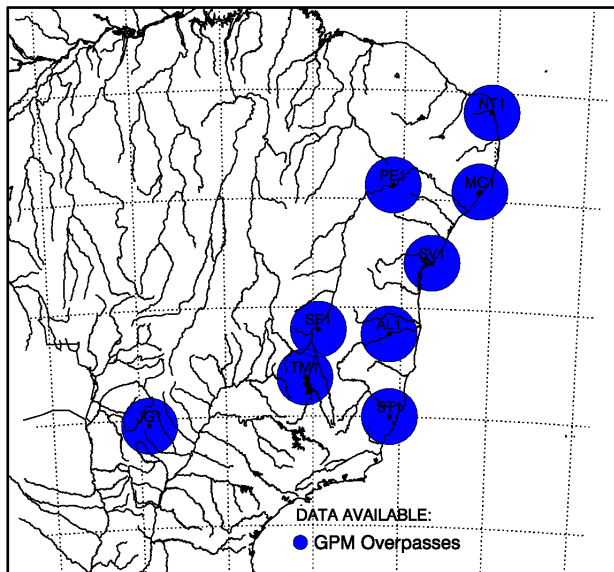


Fig 2. Brazilian GPM-GV radar sites. Blue indicates sites where only GPM overpass data are processed.

GPM GV acquires raw dual polarimetric radar data on a daily and overpass basis, which are then sorted by site, quality controlled, and calibrated. Numerous dual-polarization techniques are used to provide rain rate estimates, hydrometeor classification, and drop size distribution retrievals. In this presentation; data acquisition, operational processing, product generation, and data distribution will be discussed. A flow chart depicting the GPM GV operating procedure is displayed in Fig. 3. Data processing is conducted at NASA's Goddard Space Flight Center (GSFC) in Greenbelt, Maryland.

2. DATA ACQUISITION

Multiple methods are employed by GPM GV to retrieve raw radar data. The majority of the data retrieval process has been automated through the use of programs and scripts. Table 1 highlights the radar type, number of sites, and data acquisition time scales. This section will highlight the methods of retrieving raw radar data.

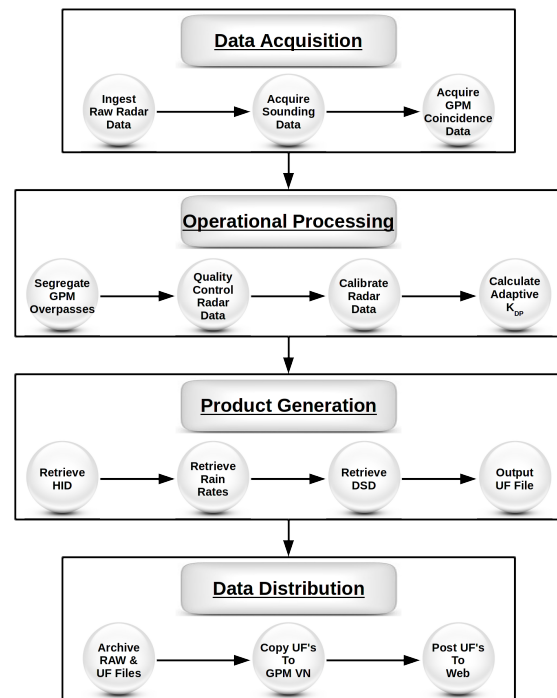


Fig 3. Flowchart of the GPM GV operating procedure for data acquisition, operational processing, product generation, and data distribution.

Radar Type	# of sites	Acquisition Time Scale
WSR-88D	66	near real time
CEMADEN	9	near real time
KPOL	1	once daily
NPOL	1	GPM overpass: near real time full data set: hand delivered
CHILL	1	GPM overpass case by case

Table 1. Radar type, number of sites, and data acquisition time scales are shown. The majority of the data are retrieved in near real time.

NOAA WSR-88D Level II data are acquired in near real time via Education and Research Consortium (ERC) NEXRAD local data manager (LDM) stream. A dedicated machine with the necessary internet2 connection ingests approximately 150GB of WSR-88D data daily from sixty-six sites. Automated scripts sort the data by site and date and lastly move it to the raw data archive.

Raw SIGMET data from KPOL are provided daily by Atmospheric Technology Services Company (ATSC). Data are obtained daily via secure copy (SCP) from Kwajalein to ATSC in Huntsville, Alabama and then to GSFC, where data are archived.

A continuous real time data feed of the

full-16-bit resolution NPOL data set is not feasible due to the high cost of transferring data through wireless networks; hence, reduced 8-bit resolution data are transferred in real time. The limited NPOL data that correspond with a GPM overpass are obtained in near real time in full-resolution. NPOL full-resolution data sets are retrieved at the radar site on portable hard drives and transported to NASA's Wallops Flight Facility (WFF) where the data are archived. A secondary archive exists at GSFC and is hosted on file transfer protocol (FTP) for public download.

Colorado State University (CSU) provides CHILL data from GPM overpasses via FTP on a case-by-case basis.

Brazil's CEMADEN radar data are acquired in near real time in Selex Rainbow format. Automated scripts retrieve, convert to UF, and archive the data at GSFC.

3. OPERATIONAL PROCESSING

Quality control, calibration, and calculation of a robust specific differential phase (K_{dp}) are critical steps to ensure high quality rainfall products. This section will detail the operational processing procedures.

GPM GV processes two data sets. The first is a subset of data that correspond to GPM overpasses - this is the GPM Validation Network (GPM-VN) data set (Schwaller and Morris 2011; Morris et al. 2015). The second is the full data set without regard to overpasses. "Full data sets" refers to the five sites that are continuously processed, two legacy sites from the Tropical Rainfall Measurement Mission (TRMM) era, Kwajalein Atoll (KPOL) and Melbourne, FL (KMLB). Three remaining sites Wakefield, VA (KAKQ); Dover, DE (KDOX); and Newark, MD (NPOL) are processed in support of the Wallops Precipitation Research Facility (PRF - Wolff et al. 2015). GPM satellite coincidence files from the NASA Precipitation Processing System (PPS) are used to identify overpass details specific to each radar. When an overpass time is within 5 minutes of the radar data time stamp and nadir distance is within 200 km, the data are segregated for processing. Automated scripts download the coincidence files and segregate the data. Approximately thirty-five GPM overpass matches occur daily.

Quality control, hydrometeor classification, and rain rate estimates use model sounding data to

identify the melting layer and ice crystals. Automated scripts download hourly model soundings from NOAA. Due to model geographical limitations we use multiple models for the retrieval of sounding data; the rapid refresh (RAP) model is used for CONUS sites; the RAP_221 model is used for Alaskan and Puerto Rican sites; the flow-following finite-volume Icosahedral model (FIM) is used for Pacific island sites; the global forecast system (GFS) model is used for Brazilian sites; and actual sounding data are used for KPOL, where the 00Z soundings are downloaded daily.

3.1 Quality Control

The removal of non-precipitating echoes from these radar data sets is a critical first step. Quality control (QC) is applied to the radar data using the NASA developed Dual Polarimetric Quality Control (DPQC) algorithm (Pippitt et al. 2013). Dual polarimetric parameter threshold modules are used to identify and remove non-precipitating echoes. Automated scripts run default QC parameters on data, the results are manually viewed and if needed QC parameters are modified. Once the QC operator determines the data are clean, the UF files are archived and we proceed to the calibration step.

3.2 Calibration

Accurate calibration of radar reflectivity is integral to quantitative radar measurements of precipitation and other radar-based applications. Calibration adjustments are only applied to NPOL and KPOL reflectivity and differential reflectivity data. Calibration adjustments are determined via the Relative Calibration Adjustment (RCA) technique (Silberstein et al. 2008; Wolff et al. 2015), self-consistency of polarimetric variables, and vertical profile (birdbath) scans. Calibration parameters are applied to the data and the resulting UF files are archived.

3.3 Specific Differential Phase

Specific differential phase (K_{dp}), the range derivative of differential phase shift (Φ_{dp}), is one of the critical parameters used for rainfall estimation and attenuation correction. Estimation of K_{dp} is a difficult task because radars do not measure Φ_{dp} directly. The total differential phase (Ψ_{dp}), which is the phase variable actually measured by the radars, contains both Φ_{dp} and measurement fluctuations. To obtain Φ_{dp} , GPM GV utilizes the adaptive estimation algorithm proposed by Wang and Chandrasekar

(2009). The algorithm is implemented at S-band to mitigate noise fluctuations and minimize the estimation errors. ψ_{dp} is processed at each range gate in complex number space to avoid phase folding and better preserves relative maximums in the peak K_{dp} . The original K_{dp} is replaced with the calculated estimate derived from Wang and Chandrasekar (2009) and placed into the data volume to be used for downstream science applications.

4. PRODUCT GENERATION

Once operational processing is completed, dual polarimetric rainfall products can be generated, rain rate estimates, hydrometeor classification, and drop size distribution retrievals. Table 2 lists the full complement of products generated and stored as fields in UF format radar data files.

Field Name	Description
ZZ	Uncorrected Reflectivity
CZ	Corrected Reflectivity
RH	Co-polar Cross Correlation (ρ_{hv})
DR	Differential Reflectivity (Z_{dr})
PH	Differential Phase (Φ_{dp})
KD	Specific Differential Phase (K_{dp})
SW	Spectrum Width
SQ	Signal Quality Index
VR	Radial Velocity
FH	Hydrometeor Identification (HID)
D0	Median Volume Diameter
DM	Mass Weighted Mean Diameter
NW	Normalized Intercept Parameter
N2	Normalized Intercept Parameter
RR	DROPS2 Rain Rate
RP	PolZR Rain Rate

Table 2. List of fields available after full GV processing

4.1 Rain Rate Estimates

Two separate rain rates estimates are calculated from the dual-polarization data; a polarimetrically tuned Z-R algorithm that adjusts for drop oscillations (PolZR - Bringi et al. 2004), and a more recent hydrometeor identification approach

referred to as the Dual-Polarization Radar Operational Processing System (DROPS2.0 - Chen et al. 2015). Fig. 4 shows the corrected reflectivity from a representative convective event that occurred on 21 June 2015. This event will be used as an example for GPM GV rainfall products.

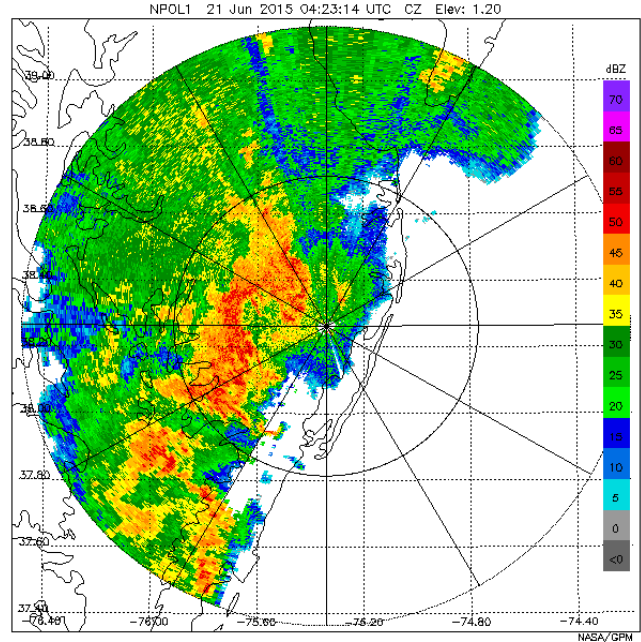


Fig 4. Quality controlled reflectivity (CZ) image from convective NPOL case on 21 June 2015. Range rings are at 50 km intervals.

4.1.1 PolZR

The PolZR rain rate estimate is derived from the polarimetrically tuned Z-R relation developed by Bringi et al. (2004). The coefficient “a” of a polarimetrically based Z-R relation of the form $Z=aR^{1.5}$ is continuously adjusted as the Drop Size Distribution (DSD) evolves in space and time, via the estimation of the normalized gamma DSD by observed values of Z_h , Z_{dr} and K_{dp} (Gorgucci et al. 2002). The rain rates generated by PolZR are placed in the RP field. An example of the RP field from the test case can be viewed in Fig. 5. Rain rates of greater than 75 mm hr^{-1} are evident in the convective cells.

4.1.2 DROPS2.0

The Dual-Polarization Radar Operational Processing System (DROPS2.0; Chen et al. 2015) supplies our final rain rate estimate. The hydrometeor classification algorithm (HCA) used within DROPS2 is based on the methodology proposed by Bechini and Chandrasekar (2015). Model soundings discussed in section 3 assist the HCA in determining hydrometeor

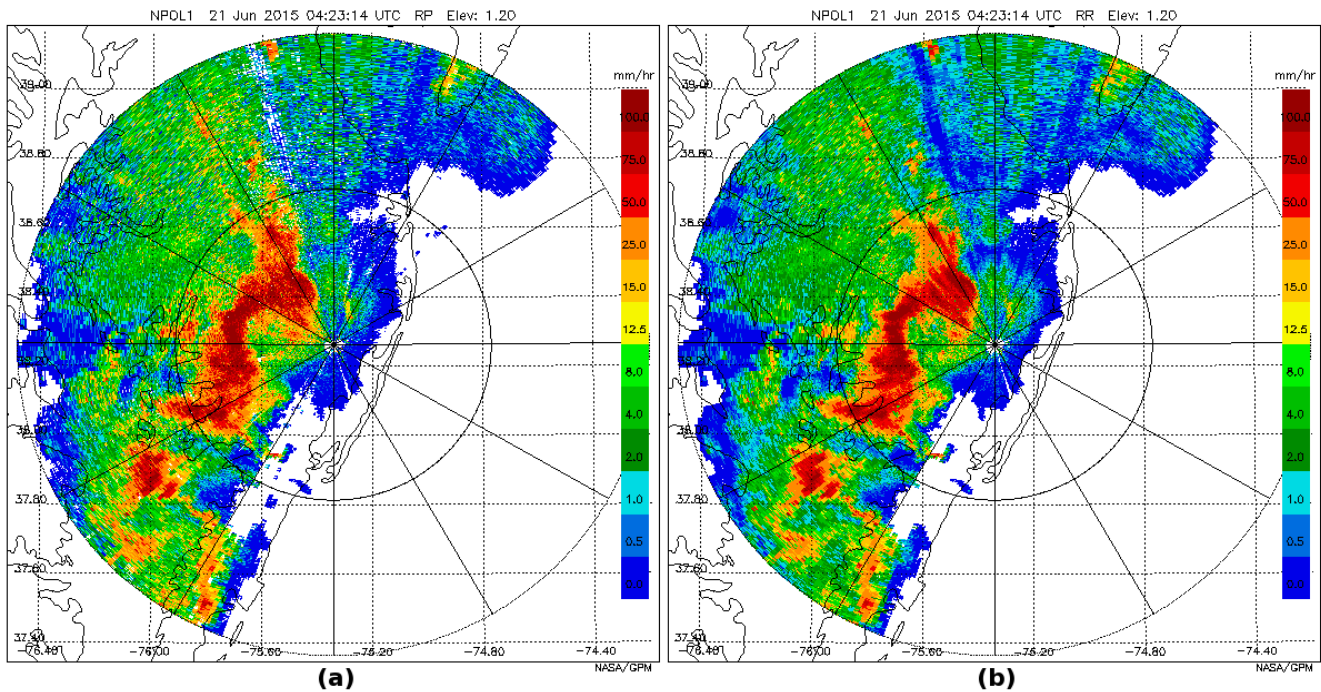


Fig 5. NPOL convective case from 21 June 2015 shows rain rate fields produced by GPM GV; (a) PolZR (RP) and (b) DROPS2.0 (RR). Both approaches identify rain rates greater than 75 mm hr^{-1} within the convective cells. The DROPS2.0 method appears visually cleaner than the other method. Range rings are at 50 km intervals.

type. The HCA utilized for the DROPS2.0 program is designed to identify very general characteristics (large drops, rain, drizzle, heavy rain) of the observed data, in order to partition areas of rain from *mixed phase or ice areas, in which no rain rate estimate is retrieved*. The rain rates generated by DROPS2.0 are placed in the RR field. An example of the RR field from the test case can be viewed in Fig. 5. Similar to the previous method rain rates of greater than 75 mm hr^{-1} are evident in the convective cells. The DROPS2.0 method appears visually cleaner than the PolZR method. The two rain rate estimates are being evaluated with Wallops PRF rain gauges from the $5\text{km} \times 5\text{km}$ dense Pocomoke grid and gauges from a 0.5° grid (Wolff et al. 2015).

4.2 Drop Size Distribution Retrievals

Four DSD retrievals are calculated. The median drop diameter (D_0) and normalized intercept parameter (N_w) fields are retrieved using polarimetrically tuned regressions via T-matrix simulations from disdrometer data collected in a wide variety of weather regimes observed in Huntsville, Alabama and Oklahoma (Mid-latitude Continental Convective Clouds Experiment MC3E; Jensen et al. 2010). Both D_0 and N_w were retrieved from a third order polynomial:

$$D_0 = 0.0215 * Z_{dr}^3 - 0.0836 * Z_{dr}^2 + 0.7898 * Z_{dr} + 0.8019$$

$$N_w = 20.957 * Z_h D_0^{-7.7}$$

Similar to the retrievals of D_0 and N_w , T-matrix simulations were used in the retrievals of the mass weighted mean diameter (D_m) and the associated normalized intercept parameter (N_w , but referred to in the data files as N_2). In addition to Huntsville, disdrometer data were collected from Wallops Island, VA and during GPM field campaigns (MC3E, IFloodS, IPHEX). Both D_m and N_2 were retrieved from a third order polynomial:

$$D_m = 0.0355 * Z_{dr}^3 - 0.3281 * Z_{dr}^2 + 1.4867 * Z_{dr} + 0.6615$$

$$N_2 = 30.93 * Z_h D_m^{-7.141}$$

The generated DSD retrievals are placed in the D_0 , N_w , D_m , and N_2 fields. An example from the 21 June 2015 NPOL case are shown in Fig. 6. and Fig. 7.

4.3 Hydrometeor Identification

The HCA utilized for the DROPS2.0 program is designed to identify very general hydrometeor characteristics; hence, GPM GV utilizes the CSU

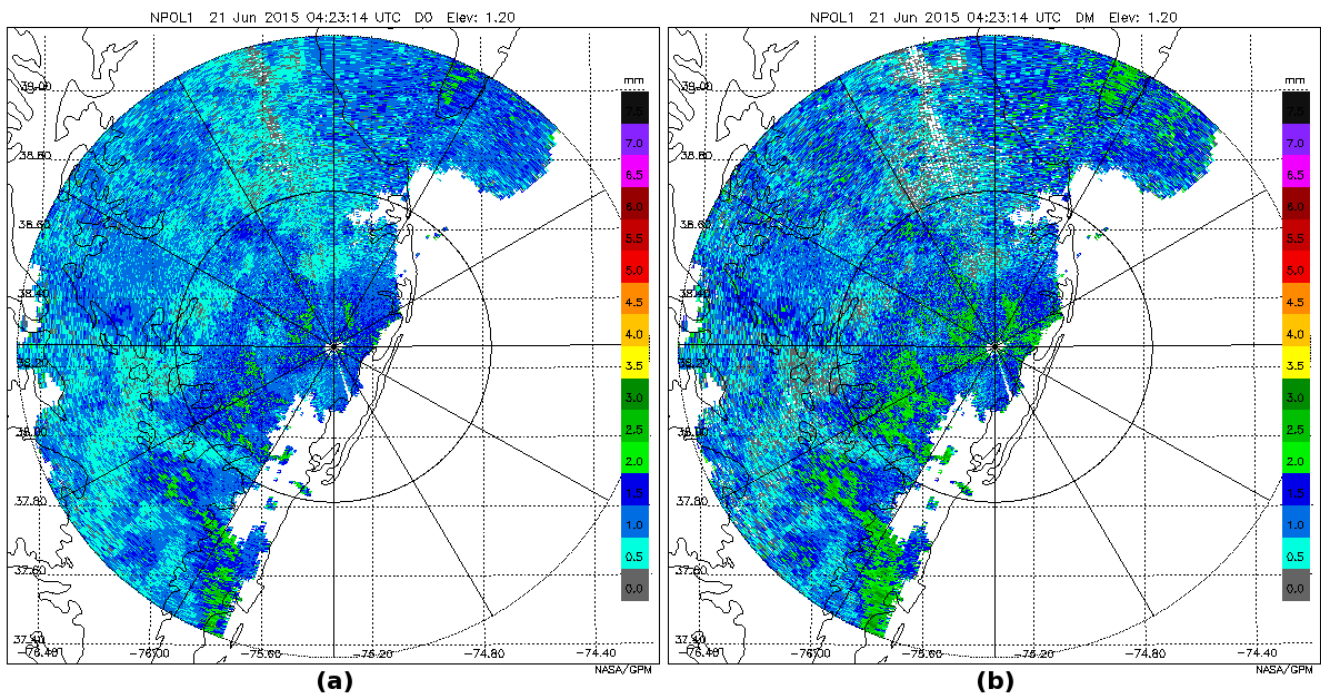


Fig 6. NPOL convective case from 21 June 2015 shows two DSD retrievals produced by GPM GV; (a) median drop diameter (D_0) and (b) mass weighted mean diameter (DM). Range rings are at 50 km intervals.

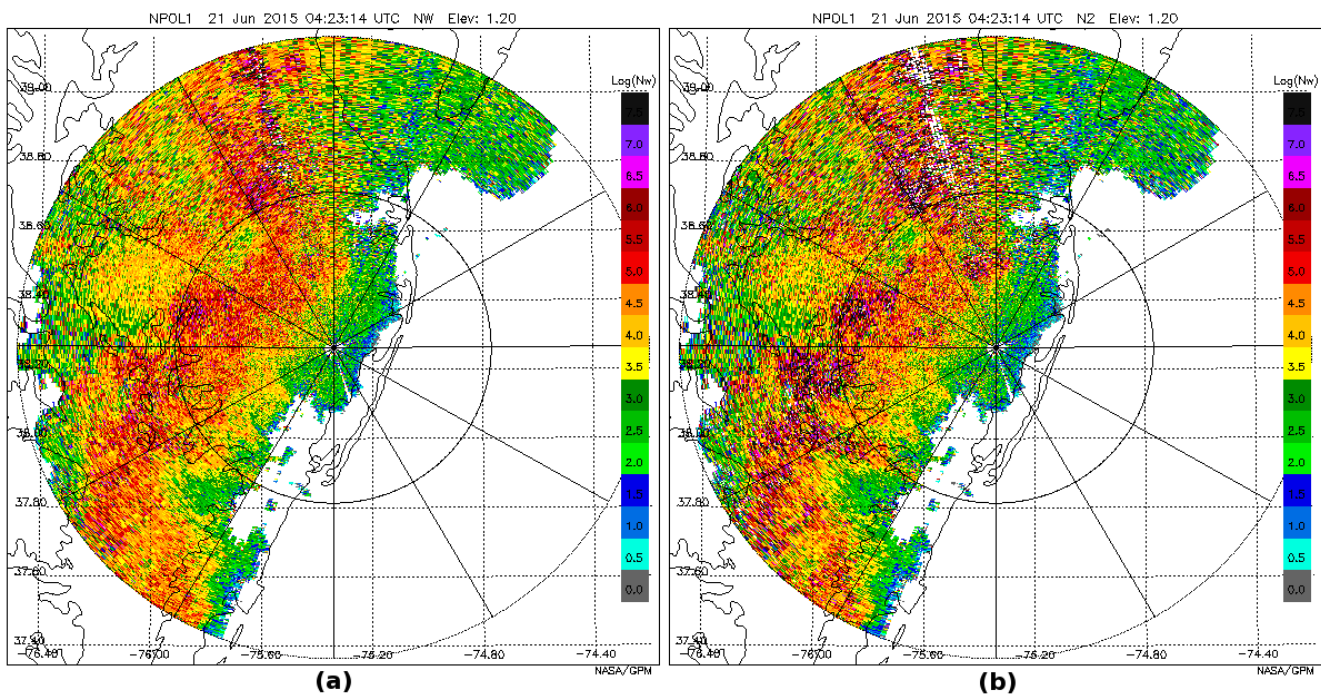


Fig 7. NPOL convective case from 21 June 2015 shows two DSD retrievals produced by GPM GV; (a) the normalized intercept parameter (NW); and, (b) the D_m associated normalized intercept parameter (N_2). Range rings are at 50 km intervals.

warm season Hydrometeor Identification (HID) algorithm to generate a more detailed hydrometeor classification. HID is a ten-category fuzzy logic-based algorithm constructed from a series of scattering simulations. Parameters for drizzle (DZ), rain (RN),

ice crystals (CR), low-density graupel (LDG), high-density graupel (HDG), and aggregates (AG) are described in Dolan and Rutledge (2009), while hail (HA), wet snow (WS) and big drop/melting hail (BD/MH) microphysical assumptions are discussed in

Dolan et al. (2013), as well as updated parameters for vertical ice (VI). Membership Beta Functions (MBF) are used to define the most probable values for each hydrometeor type as found in the scattering simulations. In addition to reflectivity (Z_h), differential reflectivity (Z_{dr}), specific differential phase (K_{dp}), and cross-correlation coefficient (ρ_{hv}), the algorithm also takes vertical temperature input from a nearby sounding (discussed in section 3) in order to limit the vertical extent of certain hydrometeor types, such as ice crystals in the rain layer, etc. The steps for fuzzy logic classification are described in detail in Liu and Chandrasekar (2000) as well as Dolan and Rutledge (2009). Each hydrometeor category is scored based on a ‘hybrid’ weighting scheme which additively weights contributions from Z_{dr} , K_{dp} and ρ_{hv} , then multiplies by the score of reflectivity and temperature. The highest scoring hydrometeor at each point is classified, resulting in the ‘dominant’ hydrometeor type within a pulse volume, mixtures are not allowed. HID categories are shown in Table 3. The generated hydrometeor identification are placed in the FH field. One example of the FH field, a mixed phase event at Dover, DE (KDOX) on 15 February 2015, can be viewed in Fig. 8. Low-density graupel, vertical ice, ice

crystal, and dry snow are identified. An example of the FH field during a 21 July 2015 convective event at NPOL can be viewed in Fig. 9. The RHI scan of this impressive 15 km convective cell shows a large area of hail aloft and an area of big drops/melting hail near the surface.

HID Category	Description
UC	Unclassified
DZ	Drizzle
RN	Rain
CR	Ice Crystals
DS	Dry Snow/Aggregates
WS	Wet Snow
VI	Vertical Ice
LDG	Low-density Graupel
HDG	High-density Graupel
HA	Hail
BD/MH	Big Drops/Melting Hail

Table 3. HID categories available in the FH field.

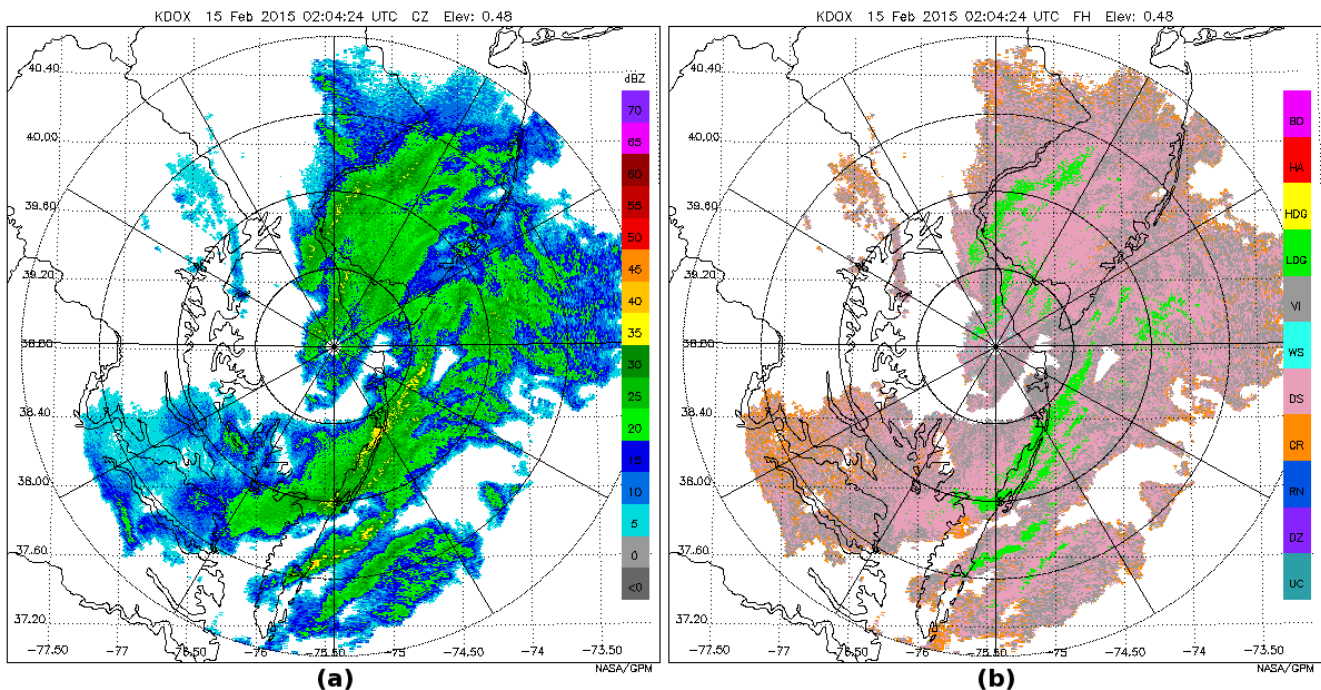


Fig 8. A Dover, DE (KDOX) mixed phase case from 15 February 2015 shows the hydrometeor identification field produced by GPM GV. (a) Corrected reflectivity (CZ) and (b) Hydrometeor Identification (FH). Low-density graupel, vertical ice, ice crystal, and dry snow are identified. HID categories are UC: unclassified, DZ: drizzle, RN: Rain, CR: Ice crystals, DS: Dry snow/ aggregates, WS: Wet snow, VI: Vertical ice, LDG: Low-density graupel, HDG: High-density graupel, HA: Hail, BD/MH: Big drops/melting hail. Range rings are at 50 km intervals.

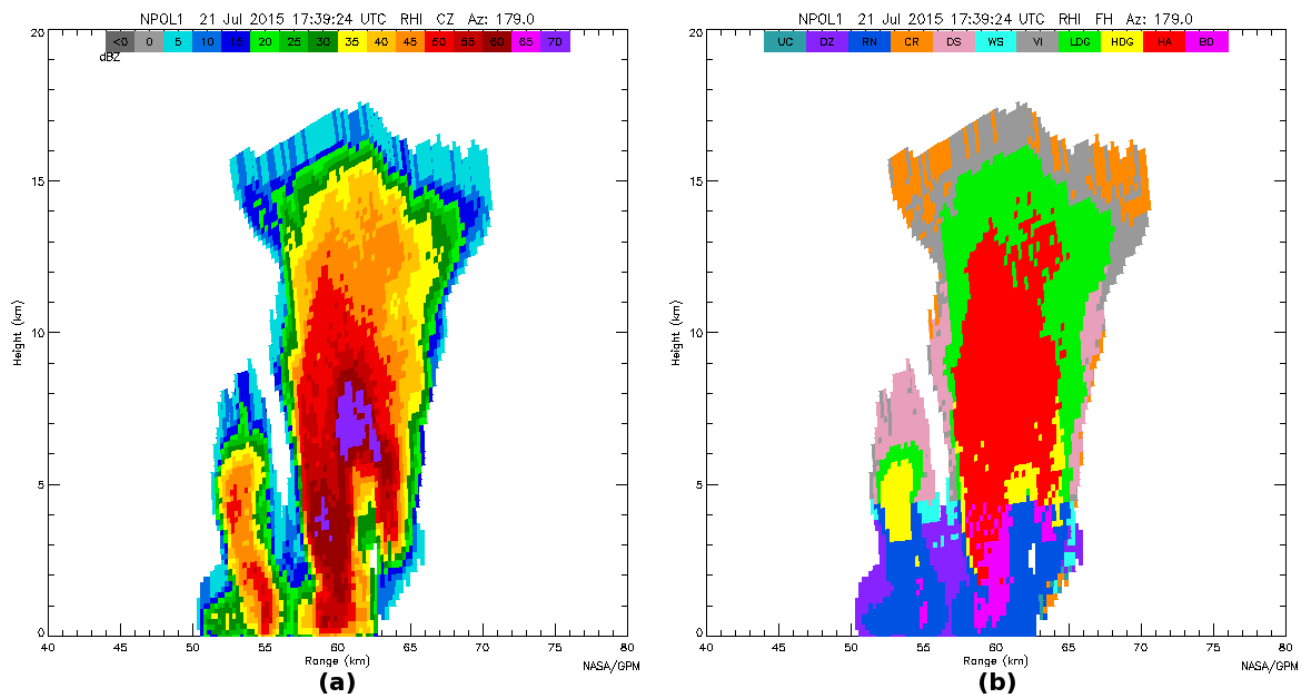


Fig 9. RHI images from a NPOL convective cell case, 21 July 2015 shows the hydrometeor identification field produced by GPM GV. (a) Corrected reflectivity (CZ) and (b) Hydrometeor Identification (FH). An impressive 15 km convective cell with a large area of hail aloft and an area of big drops/melting hail near the surface is evident. HID categories are UC: unclassified, DZ: drizzle, RN: Rain, CR: Ice crystals, DS: Dry snow/aggregates, WS: Wet snow, VI: Vertical ice, LDG: Low-density graupel, HDG: High-density graupel, HA: Hail, BD/MH: Big drops/melting hail.

5. DATA DISTRIBUTION

Final UF files are archived and GPM VN data are available to the community for science applications. GPM VN overpass and select full data set sites are hosted on public FTP and can be found through the following website:

<http://gpm-gv.gsfc.nasa.gov/Radar/>

GPM VN visualization tools that enable users to visualize the corresponding data measured by space-based Precipitation Radar (PR) and measurements collected by ground radars, can be found via:

<http://opensource.gsfc.nasa.gov/projects/GPMV/index.php>

Data requests and questions can be sent to: jason.l.pippitt@nasa.gov

6. SUMMARY

GPM GV has established an data processing

suite using a current network of 78 weather radars located in different meteorological regimes to identify errors between ground observations and GPM satellite retrievals, understand the physical basis of uncertainties, and improve both space and ground-based precipitation estimation. GPM GV has automated numerous processing procedures to streamline data flow to the community. Raw data are acquired for all sites and archived locally. Operational processing consisting of quality control, calibration, and calculation of specific differential phase is performed prior to rain rate, hydrometeor identification, and DSD retrievals. The final data are in UF format and available to the community through FTP. The resulting data is a key element in bridging the space and time gap between satellite observations and in-situ surface instrumentation such as rain gauges and disdrometers.

7. REFERENCES

Bechini, R., and V. Chandrasekar, 2015: A Semisupervised Robust Hydrometeor Classification Method for Dual-Polarization Radar Applications. *J. Atmos. Oceanic*

- Technol., 32, 22–47.
doi:
<http://dx.doi.org/10.1175/JTECH-D-14-00097.1>
- Bringi V. N., T. Tang, and V. Chandrasekar, 2004: Evaluation of a new polarimetrically based Z-R relation. *J. Atmos. Ocean. Tech.*, 21, 612-623.
- Chen, H., V. Chandrasekar, R. Bechini, 2015: An Improved Dual-Polarization Radar Rainfall Algorithm (DROPS2.0): Application in NASA IFloodS Field Campaign. *Journal of Hydrometeorology*, (to be submitted)
- Dolan B. and S. A. Rutledge, 2009: A theory-based hydrometeor identification algorithm for X-band polarimetric radars. *J. Atmos. Ocean. Tech.*, 26, 2071-2088.
- Dolan B., S. A. Rutledge, S. Lim, V. Chandrasekar and M. Thurai, 2013: A robust C-band hydrometeor identification algorithm and application to a long-term polarimetric radar dataset. *J. Appl. Met. And Clim.*, 52, 2162-2186.
- Gorgucci E., V. Chandrasekar, V. N. Bringi, and Gianfranco Scarchilli, 2002: Estimation of Raindrop Size Distribution Parameters from Polarimetric Radar Measurements. *J. Atmos. Sci.*, 59, 2373–2384. doi:
[http://dx.doi.org/10.1175/1520-0469\(2002\)059<2373:EORSDP>2.0.CO;2](http://dx.doi.org/10.1175/1520-0469(2002)059<2373:EORSDP>2.0.CO;2)
- Jensen, M. P., and co-authors, 2010: Mid-latitude Continental Convective Clouds Experiment (MC3E). U.S. DOE/SC-ARM/10-004.
- Liu H., and V. Chandrasekar, 2000: Classification of Hydrometeors Based on Polarimetric Radar Measurements: Development of Fuzzy Logic and Neuro-Fuzzy Systems, and In Situ Verification. *J. Atmos. Oceanic Technol.*, 17, 140–164.
doi:
[http://dx.doi.org/10.1175/1520-0426\(2000\)017<0140:COHBOP>2.0.CO;2](http://dx.doi.org/10.1175/1520-0426(2000)017<0140:COHBOP>2.0.CO;2)
- Marks, D. A., D. B. Wolff, L. D. Carey, and A. Tokay, 2011a: Quality Control and Calibration of the Dual-Polarization Radar at Kwajalein, RMI. *J. Atmos. and Oceanic Tech.*, 28, 181-196.
- Marks, D. A., D. B. Wolff, D. Silberstein, A. Tokay, J. L. Pippitt and J. Wang, 2011b: Availability of High-Quality TRMM Ground Validation Data from Kwajalein, RMI: A Practical Application of the Relative Calibration Adjustment Technique. *J. Atmos. and Oceanic Tech.*, 26, 414-428.
- Morris K. R., M. R. Schwaller, J. L. Pippitt, D. B. Wolff, and W. A. Petersen, 2015: Comparison of TRMM and GPM Precipitation Radars to U.S. WSR-88D Radars in the Expanded GPM Validation Network. 37th AMS Conference on Radar Meteorology, Norman, OK, September 14-18, 2015.
- Pippitt, J. L., D. A. Marks, and D. B. Wolff, 2013: Dual-polarimetric quality control for NASA's Global Precipitation Measurement (GPM) mission ground validation program. 36th AMS Conference on Radar Meteorology, Breckenridge, CO, September 16-20, 2013.
- Schwaller, M. R. and K. R. Morris, 2011: A Ground Validation Network for the Global Precipitation Measurement Mission. *J. Atmos. Oceanic Technol.*, 28, 301–319.
- Silberstein, D. S., D. B. Wolff, D. A. Marks, D. Atlas and J. L. Pippitt, 2008: Ground Clutter as a Monitor of Radar Stability at Kwajalein, RMI. *J. Atmos. Ocean. Tech.*, 25, 1492-1505.
- Wang, Y., and V. Chandrasekar, 2009: Algorithm for Estimation of the Specific Differential Phase. *J. Atmos. Oceanic Technol.*, 26, 2565–2578.
doi:
<http://dx.doi.org/10.1175/2009JTECHA1358.1>
- Wolff D. B., D. A. Marks and W. A. Petersen: 2015: General Application of the Relative Calibration Adjustment (RCA) Technique for Monitoring and Correcting Radar Reflectivity Calibration. *J. Atmos. Oceanic Technol.*, 32, 496-506. doi:
<http://dx.doi.org/10.1175/JTECH-D-13-00185.1>
- Wolff D. B., W. A. Petersen, D. A. Marks, J. L. Pippitt, A. Tokay, S. C. Tsay, A. M. Loftus, P. Pantina, V. Chandrasekar, M. Vega, R. Beauchamp, and C. M. Nguyen, 2015: GPM Radar Studies at NASA's Wallops Precipitation Research Facility. 37th AMS

Conference on Radar Meteorology,
Norman, OK, September 14-18, 2015.

8. ACKNOWLEDGMENTS

Dr. Mathew Schwaller and Dr. Scott Braun
(NASA/GSFC); PMM-GV Office Support: Bartie
Kelley, Jianxin Wang, and David Makofski